Petroleum Science 21 (2024) 3016–3028

Contents lists available at ScienceDirect

Petroleum Science

journal homepage: www.keaipublishing.com/en/journals/petroleum-science

Original Paper

Selection and application of wavelet transform in high-frequency sequence stratigraphy analysis of coarse-grained sediment in rift basin

Ling Li [a, b, c, *], Zhi-Zhang Wang [a, b], Shun-De Yin [c], Wei-Fang Wang [d], Zhi-Chao Yu [a, b], Wen-Tian Fan [a, b], Zhi-Heng Zhang [a, b]

[a] National Key Laboratory of Petroleum Resources and Prospecting, China University of Petroleum (Beijing), Beijing, 102249, China
[b] College of Geosciences, China University of Petroleum (Beijing), Beijing, 102249, China
[c] Civil and Environmental Engineering Department, University of Waterloo, Waterloo, ON, N2L5Z5, Canada
[d] SINOPEC Petroleum Exploration and Production Research Institute, Beijing, 101599, China

A R T I C L E I N F O

Article history:
Received 23 September 2023
Received in revised form
12 April 2024
Accepted 27 June 2024
Available online 4 July 2024

Edited by Jie Hao and Teng Zhu

Keywords:
Wavelet analysis
High-resolution sequence
Sedimentary cyclicity
Asymmetric wavelets

A B S T R A C T

Wavelet transformation is a widely used method in high-frequency sequence stratigraphic analysis. However, the application is problematic since different wavelets always return the same sequence analysis results. To address this issue, we applied five commonly used wavelets to theoretical sequence models to document some application criteria. Five gradual scale-change sequence models were simplified from the glutenite succession deposition by gravity flows to form the fining-upwards cycle sequences (FUCS) and coarsening-upwards cycle sequences (CUCS). After conducting theoretical sequence model tests, the optimal wavelet (sym4) was selected and successfully used with actual data to identify the sequence boundaries. We also proposed a new method to optimize the scale of continuous wavelet transformation (CWT) for sequence boundary determination. We found that the balloon-like marks in scalograms of db4, sym4, and coif4 wavelet determine, respectively, the fourth-order sequence boundary, the thick succession sequence boundaries in FUCS, and the thick succession sequence in FUCS and CUCS. Comparing the sequence identification results shows that the asymmetric wavelets had an advantage in high-frequency sequence boundary determination and sedimentary cycle discrimination through the amplitude trend of the coefficient, in which the sym4 wavelet is the most effective. In conclusion, the asymmetry of wavelets is the first selection principle, of which asymmetric wavelets are more sensitive to sediment deposition by flood flows. The match of the wavelet between the sequence is the second selection principle, in which the correlation of time-frequency impacts the accuracy of sequence surface localization. However, the waveform of the wavelet is a visual and abstract parameter for sequence boundary detection. The appropriate wavelet for lacustrine sequence analysis is the asymmetric wavelet with a weak number of side lobes. The depositional flows, depositional process, and autogenic are three sedimentary factors that influence the sequence analysis results.

1. Introduction

The coarse-grained reservoirs are drawing considerable attention recently years (Xu et al., 2018; Li et al., 2022; Yang et al., 2022). The coarse-grained , highly heterogeneity reservoirs within steep slope of rift basin mainly deposited by gravity flow, exhibiting poorly stratification, thick layers, and high gravels content (Zhang et al., 2019; Wu et al., 2020; Deng et al., 2021). Subdividing the internal architecture of coarse-grained sediments proves to be challenging due to lack of widely developed mudstone for stratigraphic correlation and complicated evolution (Xian et al., 2007; Zhang et al., 2020). Establishing a fine stratigraphic framework is the crucial for coarse-grained reservoir. Sequence stratigraphy is applied to establish the stratigraphic framework for decades years and sequence boundaries can be detected from logging data, caused by changes in the sedimentary process. The signal analysis techniques are usefully to construct high-resolution stratigraphic frameworks (Zhang and Song, 2010; Ji et al., 2013; Oliveira Santos et al., 2023).

* Corresponding author. National Key Laboratory of Petroleum Resources and Prospecting, China University of Petroleum (Beijing), Beijing, 102249, China.
E-mail address: sevendel@163.com (L. Li).

https://doi.org/10.1016/j.petsci.2024.06.020
1995-8226/

A large number of signal analysis methods are utilized in sequence stratigraphy analysis, including maximum entropy spectra analysis (Wang et al., 2002), Fourier transformation (Weedon, 2005), Hilbert transformation (Liang et al., 2019; Elkurdy, 2019), Walsh transformation (Mukherjee et al., 2016) and wavelet analysis (Yu et al., 2023; Kadkhodaie and Rezaee, 2017; Falahatkhah et al., 2021; Ge et al., 2022). Among these methods, wavelet analysis is notably prominent for its exceptional capacity to extract and amplify hidden information from non-stationary signals. Due to its ability to meet the precision demand in analyzing the sedimentary cycle and interface detection, wavelet analysis has been widely utilized in fine stratigraphic framework construction (Ren et al., 2013; Li et al., 2013). It has been widely accepted that wavelet analysis has significant advantages in sequence stratigraphy analysis (Prokoph and Agterberg, 1999; Andreas and Frederik, 2000; Zhu et al., 2018; Liang et al., 2019). Wavelet analysis has been employed for sequence division to establish the fine stratigraphic framework in coarse-grained sediments (Xia et al., 2009; Liu and Jiang, 2010; Shao, 2017). Moreover, the formation microscanner images confirmed the determination of sequence boundaries using wavelet analysis in wells where cores absent (Yu et al., 2023). The potential of wavelet analysis in sequence division within coarse-grained sediments is evident. Additionally, automatic detection and localization of sudden or gradual changes in sedimentation succession have been successfully applied in oil source rock (Andreas and Frederik, 2000). Intelligent recognition of high-frequency sequence boundaries and sedimentary cycle types is poised to become a reality soon.

Wavelet analysis has proven to be effective in obtaining refined stratigraphic framework based on the method of sequence stratigraphic, while several problems remain to be solved in this area. First challenge is the lack of clear guidance on selecting the primary parameter for wavelet optimization. This absence can result in similar sequence analysis outcomes achieved through the utilization of different optimized wavelets (Zhu et al., 2018; Wang, 2010; Fang et al., 2007). Undoubtedly, this will increase the challenge of identifying sequence boundaries in coarse-grained sediment lacking mud. In fact, the number of vanishing moments, as well as phase and amplitude of wavelets, can have different impacts on the resolution of sequence determination, which means that using different wavelets should result in varying sequence results. Furthermore, it is clear that logging curves, the sequence types records, decides the wavelet selection (Chandrasekhar and Eswara Rao, 2012). Secondly, it is important to determine which sedimentary sequence cycle patterns can be effectively distinguished by wavelets, it is particularly crucial in sequence analysis for absence cores or just partly cores wells. And this can help to reduce errors in manual cross-section correlation through sequence stratigraphic analysis. Finally, the crucial part of wavelets analysis application is how to determine specific certain scales for sequence boundary determination. The maximum average modulus of power and the frequency analysis are two generally methods (Zhang and Song, 2010; Srivardhan, 2016). Unfortunately, they failed to extend to high-frequency sequence analysis of coarse-grained sediments succession.

The main purpose of this research is to document the wavelet selection criteria in high-frequency sequence stratigraphy where coarse-grained sediments developed. A new method called the inflection of wavelet power distribution (IPD) has been proposed to determine certain scales for detecting different sedimentary cycles. Also, two symmetric and three asymmetric wavelets were first utilized to four kinds of sedimentary sequence models to optimize the best wavelet. Furthermore, the best optimization wavelet was used to determine the sequence boundaries in actual well-logging data, then the result was compared with a stratigraphic framework established based on Milankovitch information to validate the performance of optimized wavelets and the reliability of sequence identification results. Finally, the criterion of wavelet selection was concluded, and application influence factors were discussed based on the results above.

2. Geological setting

The Dongying depression is the second-largest hydrocarbon-bearing asymmetric half-graben depression located in the southeast of Jiyang subbasin in the Bohai Bay Basin of eastern China (Fig. 1a). It is subdivided into four subtectonic units: the Boxing, Niuzhuang, Lijing, and Minfeng sages. The north regional structural configuration of half-graben depression was the result of Chennan Fault cutting through the basement, causing a convex uplift in the north and a concave depression in the south to form where corresponds to the Chenjiazhuang Rise and Dongying Depression, respectively. During the basin sedimentary process evolution, a large amount of weathered coarse-grained sediments derived from Chenjiazhuang Rise were transported downward into the Dongying Depression and deposited as thousands of meters thick successions (Xie et al., 2004). The successions are comprised of Cenozoic sediments, from basal to upper, including the Paleogene Kongdian (Ek), Shahejie (Es), and Dongying (Ed) formations, Neogene Guantao (Ng) and Minghuazhen (Nm) formations as well as Quaternary Pingyuan (Qp) formation. The footwall of the Fault is composed of exposed basement rocks including granite, gneiss, and mixed granite (Lampe et al., 2012).

The steep slope zone of Dongying Depression has abundant lithology-related hydrocarbon reservoirs. The study area is located on the steep slope of Dongying Depression (Fig. 1b), which is to the north of the Minfeng sage, and the target reservoirs are developed in the fourth member of Shahejie Formation. The fourth member of Shahejie Formation belongs to the initial rifting phase in tectonic, in which thick coarse-grained sediments are intensively controlled by Faults (Li et al., 2021) (Fig. 2). To enhance exploration and development level of those reservoirs, there has been extensive use of methods for precise reservoir characterization and prediction, including the sequence stratigraphic analysis technique, which is useful in establishing a fine stratigraphic framework. The dominant sedimentary facies in the steep slope zone are deep lacustrine environments (Xiao and Chen, 2003), which include nearshore subaqueous fans, sub-lacustrine fans, turbidite fans, deltas, and alluvial fans (Fig. 2) (Zhu et al., 2018; Li et al., 2022). There are debates in stratigraphy sequence framework based on different data. Using data extracted from the Yanjia areas, Milankovitch-related sedimentary cycles were analyzed for sequence analysis and used to subdivide four fourth-order sequences which were verified by Formation Micro Imaging (FMI) data (Song et al., 2012). However, five fourth-order sequences were subdivided based on the sediments of Shengtuo areas next to the eastern Yanjia areas (Shao, 2017). Although the sequence division has conflicts, FMI-based sequence result is a reliable stratigraphic framework that we can compare with to verify the ability of optimization wavelet. Besides, three medium-term and eleven short-term cycles were subdivided according to the cores and logging data where sampled areas located eastern of Shengtuo areas (Shi, 2009).

3. Method

3.1. Continual wavelet analysis

Wavelet analysis uses a decaying, finite-length wavelet function to replace the infinite trig functions used in Fourier transforms,

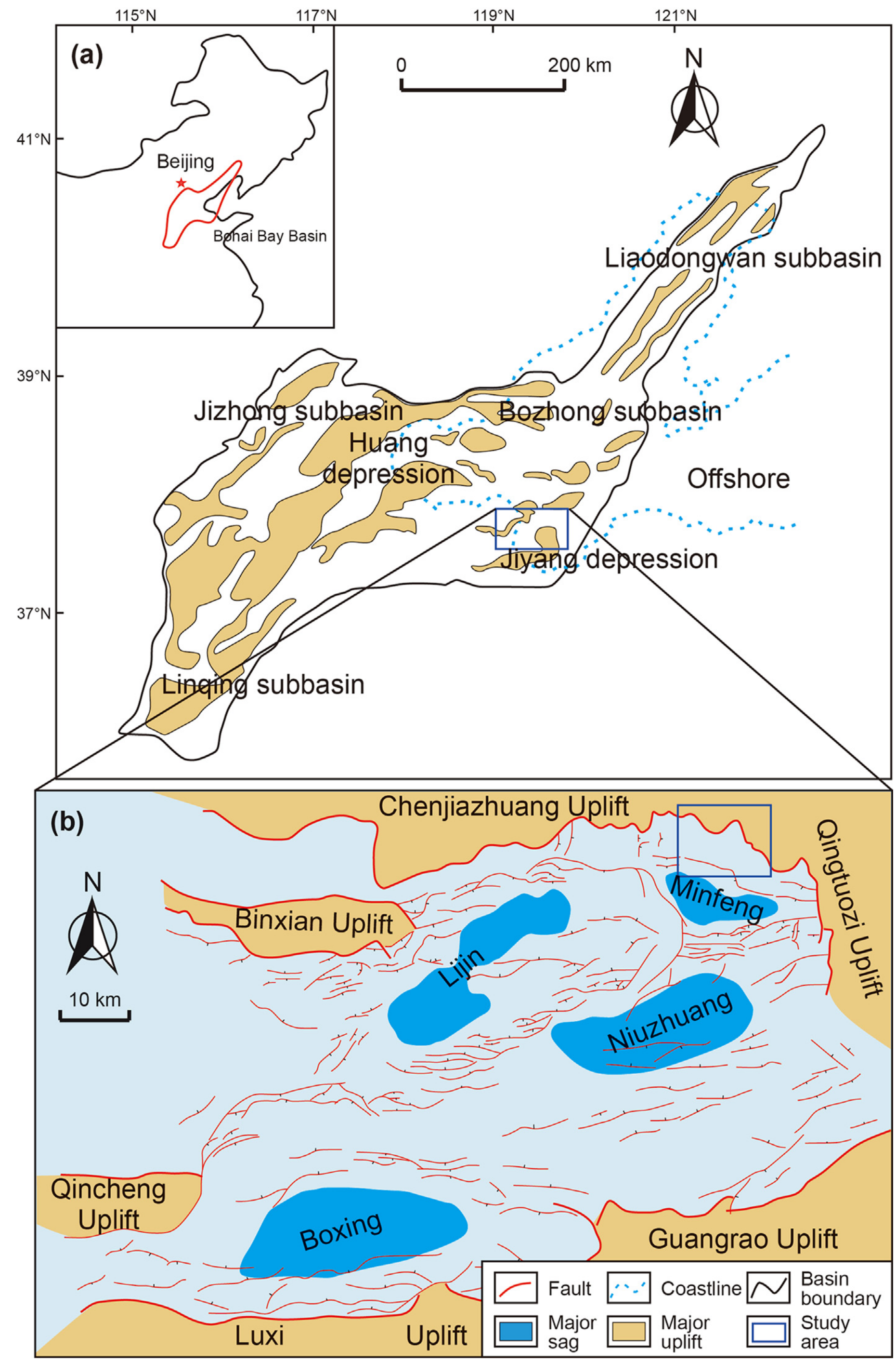

Fig. 1. **(a)** Location of the Bohai Bay Basin. **(b)** Location of the study area in the Dongying Depression.

allowing for the representation of all frequencies and more accurate time localization. (Strang, 1993). In general, three models are commonly used for the wavelet analysis: Continuous Wavelet transformation (CWT), Discrete Wavelet transformation (DWT), and Discrete-time Wavelet transformation (DTWT). The CWT is a filter transformation that converts a signal from the time domain to the time-frequency domain using sweep and convolution function (Guido et al., 2020). The results of the transformation highly depend on the special function known as the wavelet function or mother function. And a slightly amount spatial shift in the wavelet function generates equivalent shift in the transformed domain. Thus, the changes in logging data can be effectively captured. However, the DWT and DTWT analyze the signal by sequentially decomposing the input data into ideally layers based on powers of 2 (Guido, 2022). Although it can analyze the low frequency of signal, this led to the lack of sufficient precision in determining the specific scale used for locating sequence interfaces in sequence analysis. Moreover, from a signal analysis perspective, low-frequency information is not crucial for high-resolution sequence analysis. The main purpose is to explore the application criteria in high-frequency sequence stratigraphy. Therefore, CWT is used for well logging sequence analysis. The mathematical expression of CWT

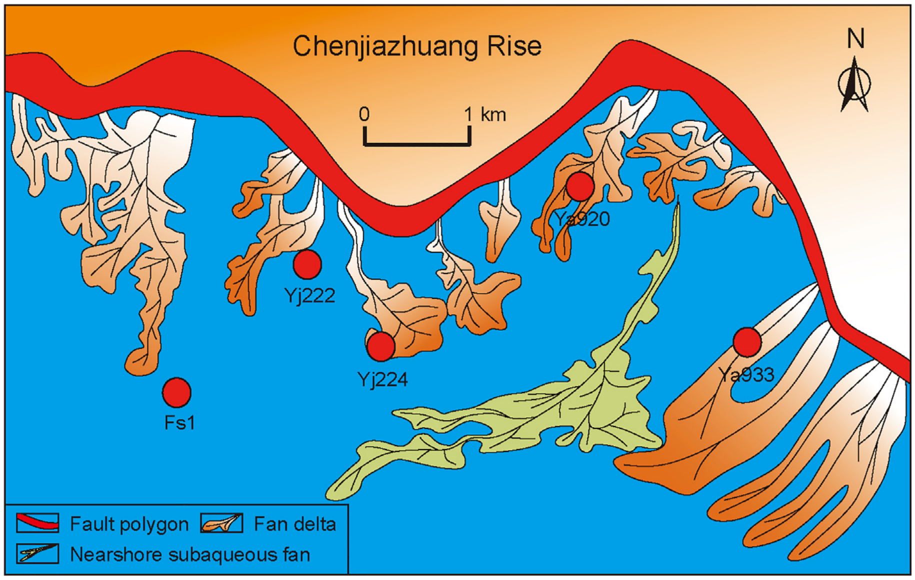

Fig. 2. Sediment systems distribution during the fourth member of Shahejie Formation deposits (Li et al., 2021).

formula is written as follows (Grossmann and Morlet, 1984); (Daubechies, 1990):

$$\mathrm{WT}(a,\tau)=\frac{1}{\sqrt{a}}\int_{-\infty}^{\infty} f(t)*\Psi\left(\frac{t-\tau}{a}\right)\mathrm{d}t \quad (1)$$

The input signal is $f(t)$ and the wavelet function is $\frac{1}{\sqrt{a}}\Psi\left(\frac{t-\tau}{a}\right)$. Where a>0 represents the scale that controls the stretching or compressing scaling of wavelet function, determines the sedimentary cycle that is analyzed in logging data and τ denotes the shift of the center of the analysis window to a location, governing the translation of the wavelet function (Prokoph and Agterberg, 2000). Scale, a, corresponds to the frequency (inverse ratio), and shift, τ, corresponds to the time shift factor. They make it possible to gradually analyze the signal over time, capturing signal details at every frequency. Thus, the specific sequence boundaries associated with portions of the logging signal are conveniently captured when frequencies are determined.

Scalogram and coefficient are two ways to use in sequence analysis (Liu and Jiang, 2010). The scalogram is an effective way to demonstrate scale (frequency) distribution, making it useful in identifying sedimentary cycle (Rioul and Vetterli, 1991). Generally, the color of scalograms changes reflect changes in frequency as the indicative mark for sequence interface. By observing the amplitude tendency inflection of the coefficients at the appropriate scale of CWT, it's possible to accurately determine sequence boundaries.

3.2. Inflexion of power distribution

Simplistically, a third-order sequence cycle is composed of two fundamental sequence patterns, of which finning-upward cycles sequence (FUCS) and coarsening-upward cycles sequence (CUCS) in steep slope of rift basin (Li et al., 2019). The large, medium, and small-scale combinations of the FUCS and CUCS correspond to long-term, middle-term, and short-term cycle patterns, and stack each other together to form the entire sequence. The accumulation of power in FUCS gradually decreases, while in CUCS it increases. An inflection of power distribution (IPD) occurs between the two sequences, indicating the transition between them. After performing continuous wavelet transform (CWT) on the data, the power of each scale (frequency) is sequentially displayed. Inflection points corresponding to each scale can then be used to determine the sequence boundaries and discriminate sedimentary cycle patterns based on the power tendency of the signal.

3.3. Sequence models

The sedimentary deposits are mainly two types of deposits: debris flow deposits and flood flow deposits (Cao et al., 2018; Yang et al., 2019, 2020). This leads to the form inverse and normal rhythms in the logging facies, respectively. Five basic difference scale parasequences represented by varying thickness were designed to construct the theoretical third-order sequence models, in which inverse sedimentary cycle represent debris flow deposits, and normal sedimentary cycle represent flood flow deposits (Fig. 3). Theoretical third-order sequence models were divided into two parts: the lower part corresponds to coarsening-upward cycle parasequence sets and the upper part corresponds to fining-upward cycle parasequence sets or vice versa (Fig. 4). Each middle-term cycle was composed of three parasequences sets with regular scale change. As a result, a fourth-order sequence boundary was formed between the two middle-term cycles, while fifth-order sequence boundaries were formed between each parasequence set. Furthermore, sixth-order sequence boundaries were formed between the parasequences. This paper focuses on the discussion of the first model, which includes both sudden interruptions and gradual changes in parasequences and is close to the actual sequence (Fig. 4a). The parasequences detailed data is listed in Table 1, where each sample point corresponds to a length of 0.125 m in well-logging. The 10 m thick mudstone separates two sedimentary cycles, which the top of the mudstone can be viewed as fourth order sequence. The internal sequence surface of two parasequence sets are fifth-order sequence and thickness of two mudstone layers of fifth-order sequence is 0.25 m and 0.5 m, respectively. The noise models, 20 dB and 24 dB, were used to test the anti-noise performance of wavelets to determine the reliability of wavelet-based sequence division for general well logging data. The thickness of parasequence sets B and E are the average thickness of the gravity flow-dominated succession in Dongying Depression, and the application of CWT mainly focus on these two parasequence sets.

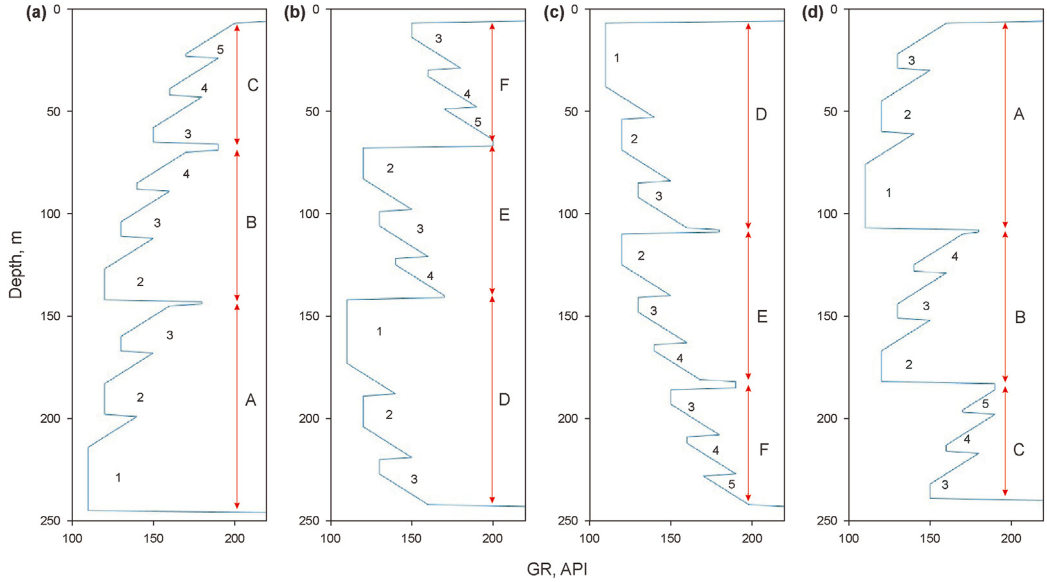

Fig. 3. Four fundamental classifications of parasequence sets. **(a)** and **(b)** are the fining-upwards cycle sequence models deposition by flood flow and debris flow, respectively; **(c)** and **(d)** are coarsening-upwards cycle sequence models deposition by flood flow and debris flow, respectively.

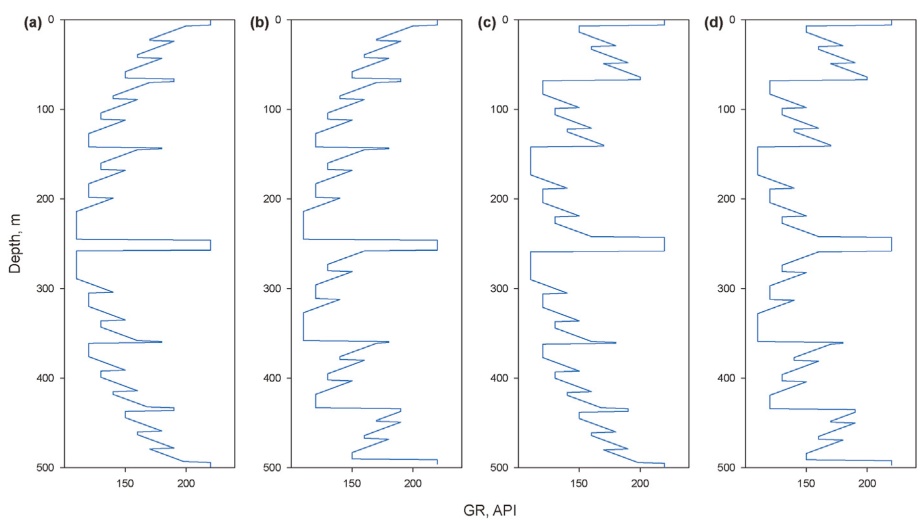

Fig. 4. Four three-order theoretical sequence models, of which 4a model is used for the presentation because it is close to the actual model.

Table 1
Theorical data of parasequence model.

Parasequence	A			B			C			D			E			F		
	1	2	3	1	2	3	1	2	3	1	2	3	1	2	3	1	2	3
Sandstone log value	110	120	130	120	130	140	150	160	170	110	120	130	120	130	140	150	160	170
Sandstone thickness	32	16	8	16	8	4	8	4	2	48	32	24	16	8	4	8	4	2
Succession thickness	48	32	24	32	24	20	24	20	19	48	32	24	32	24	20	24	20	17
Sandstone: Succession ration	66.67	50	33.33	50	33.33	20	33.33	20	10.53	66.67	50	33.33	50	33.33	20	33.33	20	11.76

The effectiveness of wavelet-based sequence analysis was evaluated by calculating the absolute error to optimize the best wavelet for sequence analysis. Additionally, the ability to distinguish different types of sedimentary cycles was used as a secondary factor for assessment. Three widely used asymmetrical wavelets and two symmetry wavelets (Fig. 5) were applied for comparison and analysis of the resolution of results.

4. Results

(1) The fifth-order sequence boundaries were identified using scalograms and coefficients from all wavelets tested in the pure model, except for the Mexhat wavelet (Fig. 6). The absolute errors of all wavelets increased with depth, where sym4 had the best performance (Fig. 7). The sequence

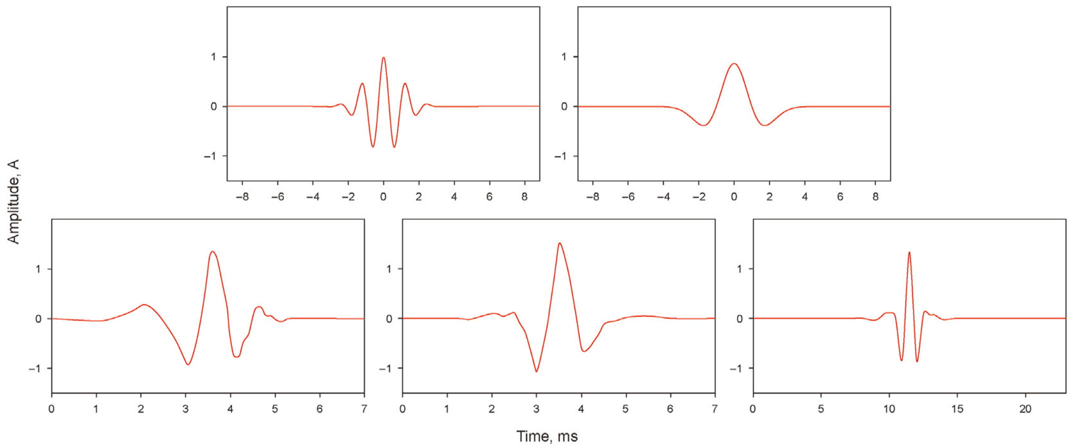

Fig. 5. Waveforms of five waveles: Morlet and Mexhat, db4, sym4, coif4, respectively (from left to right).

boundaries were determined on the scalogram by identifying obvious balloon-like marks composed of dark color (Fig. 6a). The scalogram of db4 wavelet presents balloon mark between the FUCS and CUCS (fourth-order sequence). Sym4 wavelet presents balloon mark in the thick FUCS (fifth-order sequence), but not in CUCS. Coif4 wavelet presents balloon marks in both thick FUCS and CUCS, but the thin sequence boundaries between parasequence sets BC and parasequence sets EF (fifth-order sequence) are poor. Morlet wavelet just presents one balloon mark which indicates sequence boundary between FUCS and CUCS (fourth-order sequence boundaries). Mexhat produces one balloon mark between FUCS and CUCS and low sequence resolution in internal sequences. The fifth-order sequence boundary marks were formed and indicated by circular bands composed of dark-colored stripes, which were aggregated on the scale of parasequences set. The height of the black stripes clustered together can be used to determine the rise or fall of the sedimentary base-level by scalograms of asymmetric wavelets (Fig. 6a).

And the symmetric wavelets indicate sedimentary cycles by amplitude tendency of coefficient (Fig. 6b), of which the Morlet wavelet is the most effective and can be used to determine sequence type of whether it is FUCS or CUCS. Within a single parasequence set, the sixth-order sequence boundary can be detected using asymmetric wavelet coefficients (Fig. 6b).

(2) The fifth-order sequence boundaries were still determined by scalograms of all wavelets. The balloon-like marks were still shown in scalograms of noisy models without significantly different from the pure model (Fig. 8), which implied noise has little influence for the scalograms. The fifth-order sequence boundaries were partly determined by the amplitude tendency of coefficients, in which the symmetric wavelets failed for all fifth-order sequence boundaries (Fig. 9b and c). In noisy models, the accuracy of the sequence discrimination resulting from coefficient amplitude tendency of optimal scale decreased when signal-to-noise ratio (SNR) decreased from 24 dB to 20 dB (Fig. 9b and c). The wavelets show better performance in 24 dB noisy model test. Although the sym4 wavelet is less useful than Morlet in sedimentary cycle indication, it is better in high-order sequence boundary determination. The identification ability of asymmetric wavelets is higher compared to symmetric wavelets, as observed from the power acceleration after CWT. (Fig. 9a). The sym4 wavelet is most suitable for sequence boundaries determination according to the results of absolute errors (Fig. 10).

(3) The results of actual data indicate that asymmetric wavelets perform better than symmetric wavelets (Fig. 11), in which sym4 wavelet is the best wavelet and has the highest degree of correlation to the Milankovitch-based stratigraphic framework. The coefficient indicates the peak amplitude around the depth at 3400 m and 3600 m, respectively, which are two middle-term cyclic boundaries (Fig. 11). The two short-term sequence boundaries between middle-term sequence can be indicated by the coefficient and accurately demarcated. The top short-term sequence localization lacks accuracy, and the bottom short-term sequence boundary cannot be identified under middle scale. There are some differences in short-term cycle results (Fig. 12).

5. Discussion

5.1. Asymmetric determines the ability to detect sequence boundary

Because the waveform of Morlet wavelet is similar to the periodic sinusoidal function, it has been applied to analyze the marine sedimentary cycle (Prokoph and Agterberg, 2000) and sequence boundaries which discontinues and gradually changings are both can be discriminated (Andreas and Frederik, 2000). However, it still has limitations in discriminating sedimentary cycle patterns. Rivera (Rivera et al., 2004) has pointed out that asymmetric wavelet may discriminate FUCS and CUCS.

Due to the large number of lacustrine sequences are asymmetric (Wei et al., 2010; Zheng et al., 2003; Zheng and Peng, 2002; Fu et al., 2005; Liao et al., 2010; Liang et al., 2019), asymmetric wavelet is suitable in lacustrine sedimentary sequence boundary detection. And the sequence division results indicate asymmetric wavelets performed better than symmetric wavelets. Moreover, the power acceleration of CWT results indicated asymmetric wavelet shows more sensitive detection since the power inflection point is still detected on small scale, such as power acceleration of db4 and Morlet (Fig. 8a). Thus, asymmetry should be the first principle for wavelet selection in lacustrine sequence analysis. Furthermore, Chandrasekhar has (Chandrasekhar and Eswara Rao, 2012) pointed out that the match between the shape of wavelet and the well-log

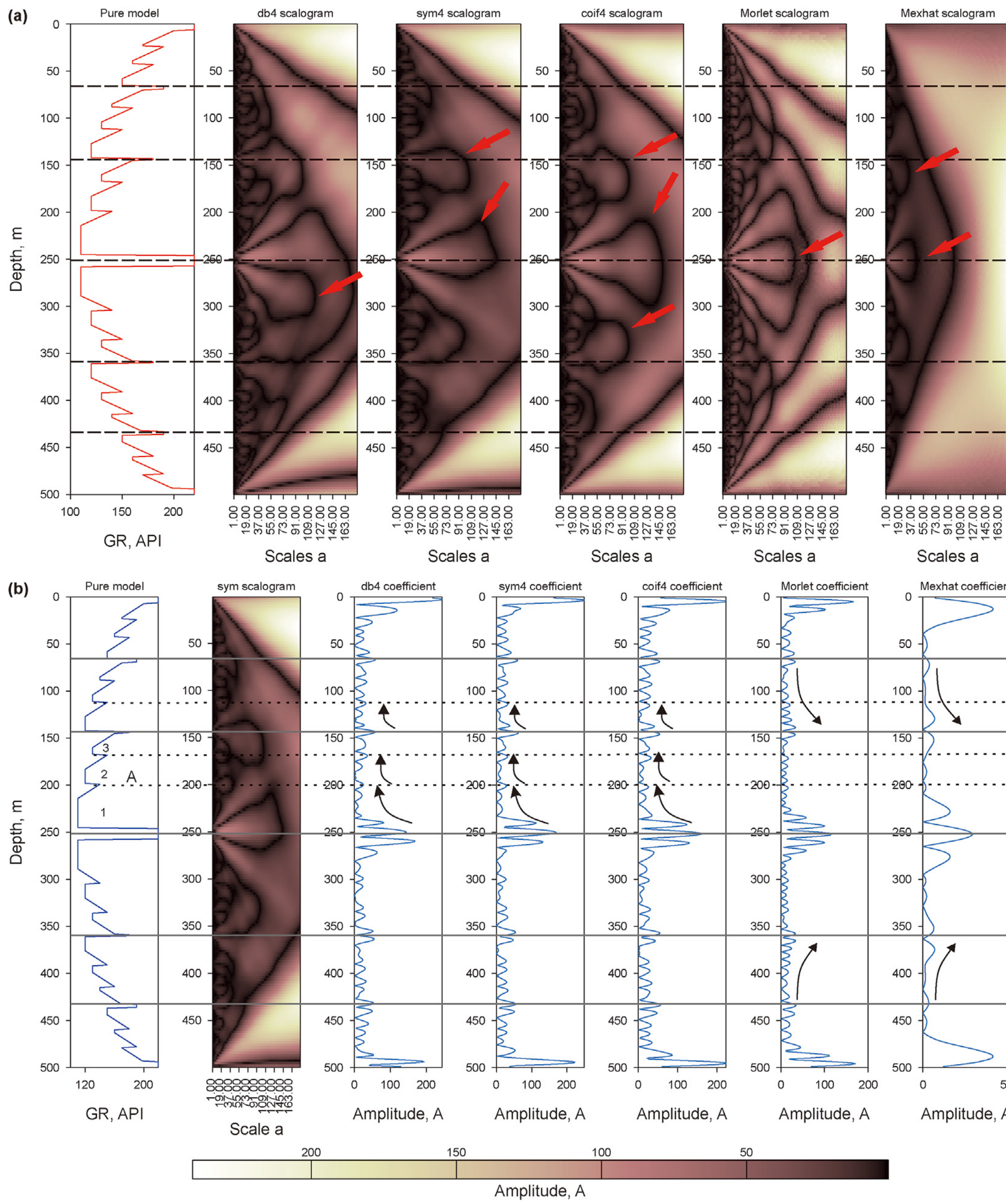

Fig. 6. The sequence boundary detective results by wavelets in pure model. **(a)** The scalogram of all wavelets sequence determination results in pure model. The balloon-like marks presented by asymmetric wavelets can detect the sequence boundaries; symmetric wavelets can hardly detect the sequence boundaries without balloon-like marks. **(b)** The coefficients of all wavelets sequence determination result in pure model. The tendency of amplitude can also be used to indicate the sedimentary cycle, in which symmetric wavelets are better in fifth-order sequence and asymmetric wavelets are better in sixth-order sequence. The black lines are the fifth-order sequence boundaries, and the black dotted lines are sixth-order sequence boundaries.

data influenced the resolution of sequence division. Visually, the waveforms of the three asymmetric wavelets had correlations with sequence trend presented in GR. When the wavelets have no correlation to the sequence, the low resolution sequence results obtained, such as the Morlet and sym2 applied to three wells in Bombay High oil field (Chandrasekhar and Eswara Rao, 2012).

Additionally, the absolute errors are larger around sequence surfaces developed in thicker sedimentary recycles compared to thinner ones. (Fig. 10). The thickness of sedimentary recycle impacts the accuracy of locating sequence boundaries. The thicker of sedimentary recycle, the larger time duration in the signal. Mathematically, the improper flotation from time to frequency domain can be caused by the nonlinear responses of wavelet function, but Symmlets and Coiflets are almost linear responses. This means using the Sym4 or Coif4 wavelet will make the time localization of the signal more precise (Guido, 2017). The correlation of time-frequency responses affects the accuracy of sequence identification. This is evident in the distinct results obtained from the db4 and sym4 wavelets, despite their high correlation with the lacustrine sequence. The match of wavelets and sequence relates to accurate sequence boundary determination and sedimentary cycle discrimination, which should be the second principle for wavelet selection. And the correlation of time-frequency impacts the accuracy of sequence surface localization. However, the sidelobe of the wavelet function also has an effect.

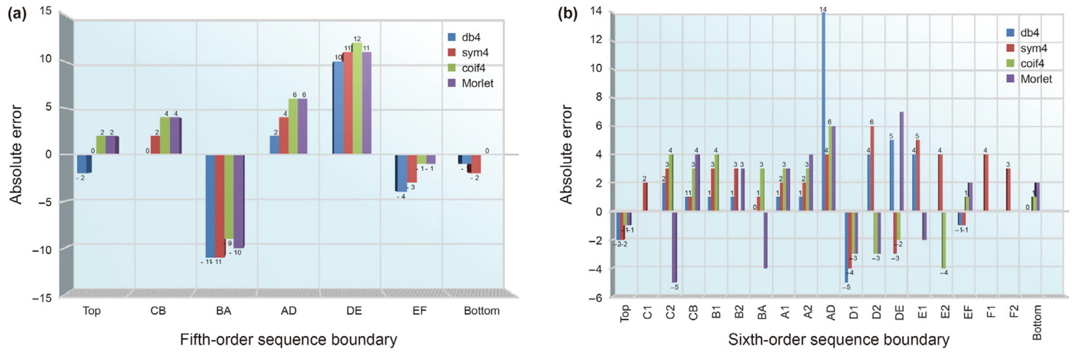

Fig. 7. The absolute errors of sequence boundaries determination for pure model. **(a)** The absolute errors of fifth-order sequence boundaries determination by four kinds of wavelet functions. **(b)** The absolute errors of sixth-order sequence boundaries determination by four kinds of wavelet functions. The absolute errors in wavelet analysis for determining sequence boundaries are larger around the thick sedimentary recycles than thin recycles. Sym4 wavelet has best performance in FUCS. Among five wavelets, the Sym4 wavelet performs the best in FUCS.

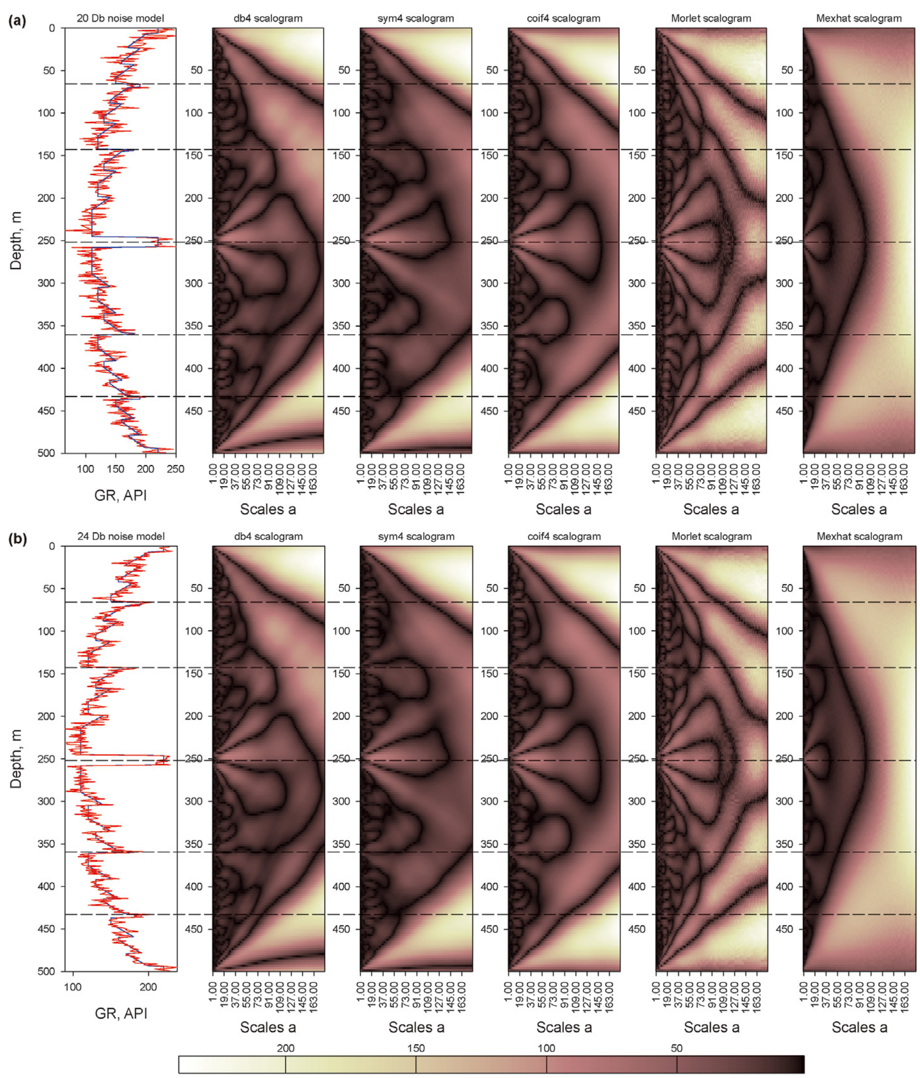

Fig. 8. The scalograms of all wavelets sequence boundaries determination for 20 dB and 24 dB noisy model. The results are similar for the two noisy models. The black dotted line is the fifth-order sequence boundary.

5.2. The development of sidelobe influence the resolution

In seismic data processing, suppressing side lobes of the wavelet can greatly improve the resolution of the seismic data to present detailed more clearly (Huang et al., 2007; Karslı and Dondurur, 2013). However, to detect certain sequence interfaces in a logging

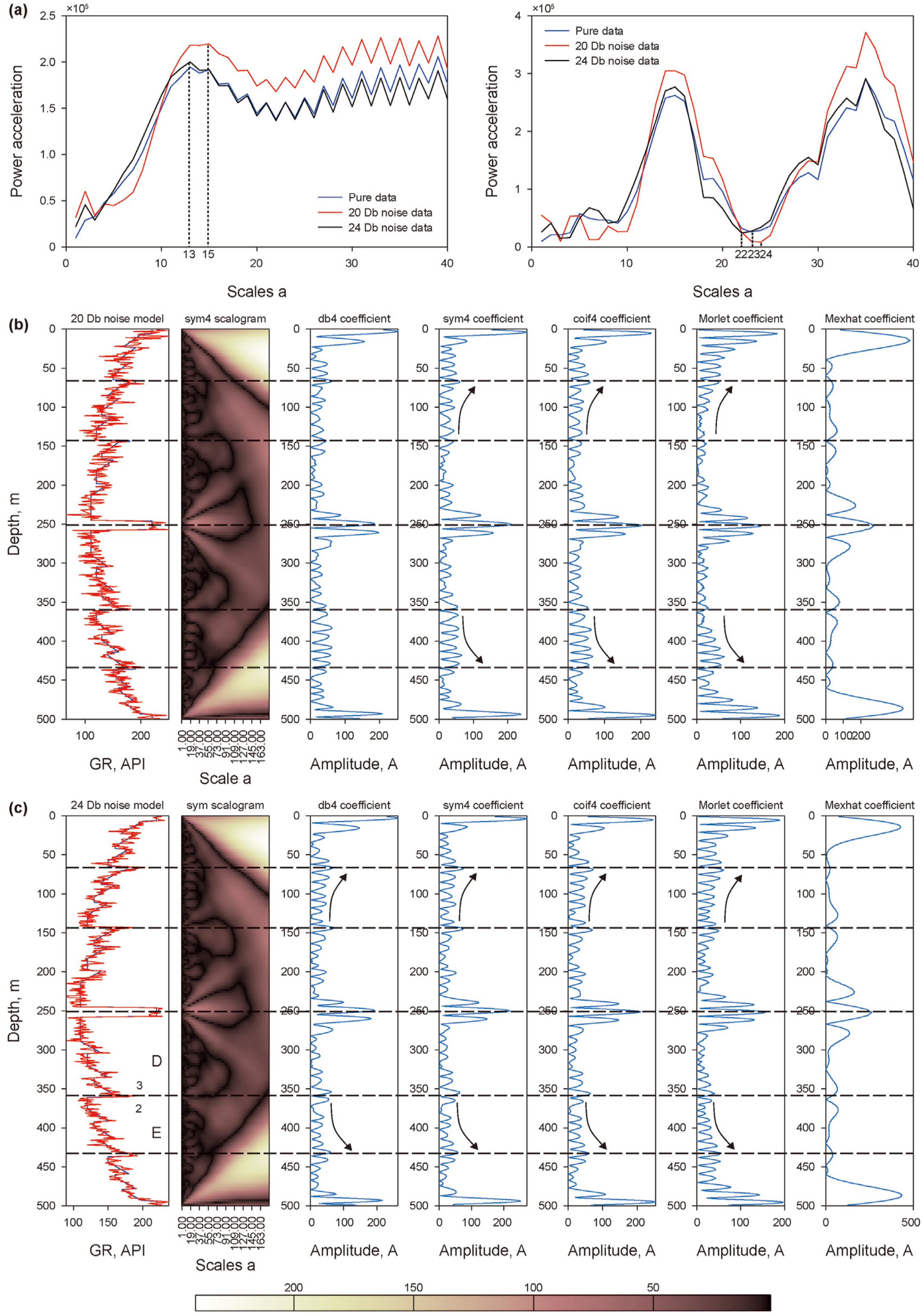

Fig. 9. **(a)** The power acceleration of db4 (left) and Morlet (right) wavelet. The asymmetric wavelet is more sensitive to detect sedimentary cycle on a small scale. **(b)** The optimal scale coefficient of all wavelets in 20 dB noisy model **(c)** The optimal scale coefficient of all wavelets in 24 dB noisy model. The wavelets have better performance in sedimentary cycle discrimination in 24 dB noisy model. The black dotted line is the fifth-order sequence boundary.

data, it may be necessary to allow for the development of side lobes. The order of sequence is related to thickness, i.e., the higher the frequency, the thinner the mudstone thickness, and they are weaker amplitude in the signal for high frequency sequence. The use of wavelet transforms in sequence analysis is to extract and amplify the cyclical and interface information in logging signals to assist in sequence analysis. In high-frequency sequency analysis, the primary challenge is maintaining signals related to third-order

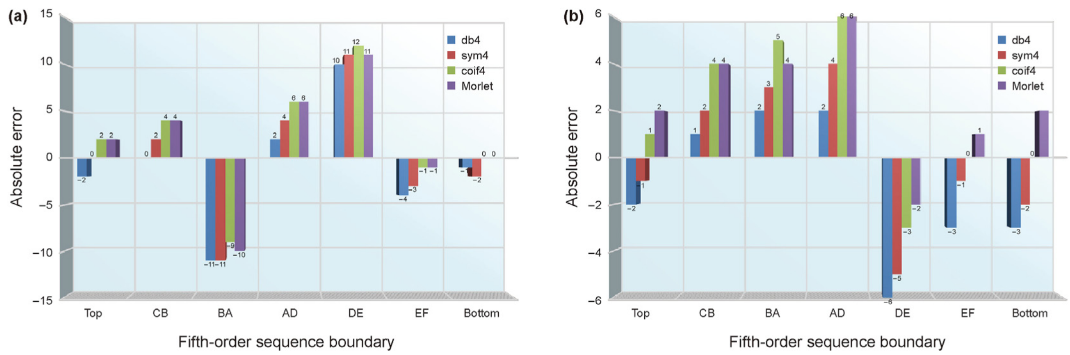

Fig. 10. The comparison of wavelet sequence analysis in noise models. **(a)** Absolute error of fifth-order sequence boundary identification in 20 dB noise model. **(b)** Absolute error of fifth-order sequence boundary identification in 24 dB noise model. Based on the error distribution, the 24 dB noise model exhibits higher identification accuracy.

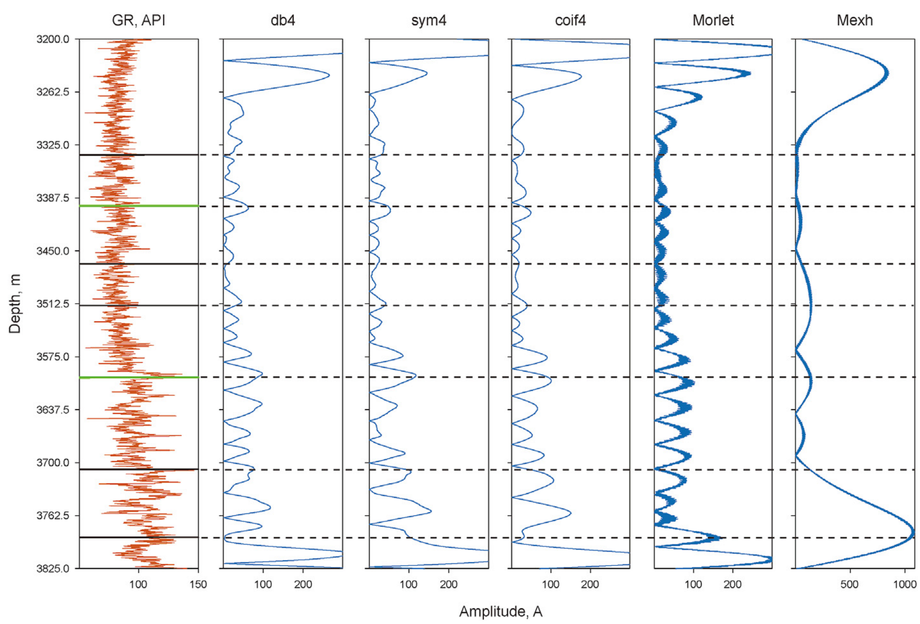

Fig. 11. The sequence determination comparison by wavelet and Milankovitch-based information. The middle-term sequence boundaries (green lines) match well and short-term sequence boundaries (black lines) also highly correlation.

sequence surfaces while amplifying weak signals related to the fifth-order sequence surfaces. Obviously, different wavelets have different detection capabilities (Kulesh et al., 2008). According to theoretical model results, higher development of side lobes (Morlet) weakens the ability to identify high-order sequence interfaces. However, the features of high-order sequence interfaces cannot be amplified without side lobes (Mexhat). Therefore, for high-frequency sequence, the wavelet with several weak side lobes would be more effective comparing the results of db4 and sym4.

5.3. *Accurate result requires high-quality data*

As wavelet is widely used in sequence analysis, it is not clear whether noise process is necessary or not as some data have been processed but some were not (Akhilesh, 2012; Pan et al., 2008). In this paper, the impact of noise volume increases when higher order sequence needs to be detected. Noisy model tests indicate that 24 dB is the threshold: noise processing is not necessary when the SNR of GR data is higher than 24 dB. Such a high-quality data is rarely found in coarse-grained sedimentary reservoir data. Undoubtedly, noise is random and impossible to clean up and would influence the high-order sequence detection.

On the other hand, autogenic is also random and internal property in high-frequency sequence. Normally, the sixth-order sequences are influenced by autogenic which is an internal property not controlled by four mainly sequence factors but flows itself (Huang et al., 2007; Ji et al., 2013). The noise and autogenic signals cannot be separated and processed independently. Part of noise can be viewed as an autogenic information under allogenic constraints when Gaussian noise is added to synthetic data, such as noise developed around points 400 (Fig. 9c). Although, the test models containing noise and autogenic are ideal for comparison and analysis, it is impossible to extract noise from signals. What we can do is access the data quality by SNR.

5.4. *The influence of deposition*

The asymmetric wavelets are sensitive to flood flow deposits. Debris flow sediments are generally sudden discontinuous, which are favorable depositional characteristics for sequence boundaries determination by CWT (Richard and Brac, 1988; Choudhury et al., 2007; Arabjamaloei et al., 2011). The asymmetric wavelets should

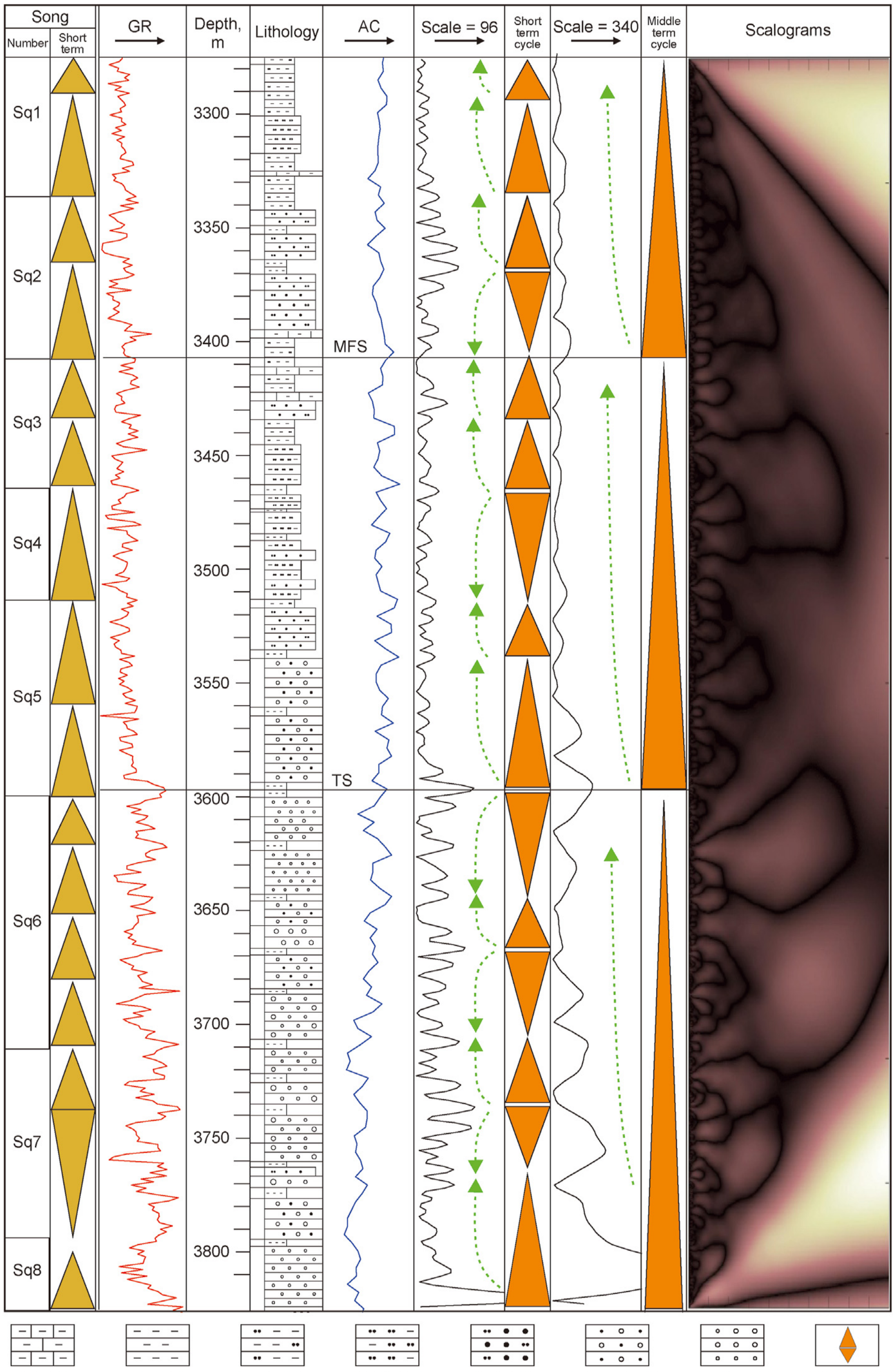

Fig. 12. The comparison of sequence determination by sym4 wavelet and Milankovitch-based sedimentary cycle (left) from Song et al. (2012). The result of Song is resulted from the well located in the Yanjia area.

have better sequence determination performance in lower than upper. However, the absolute errors of sequence determination in the lower are bigger than upper. Even the best wavelet has poor performance in debris flow deposits. Moreover, the actual data results also indicate that asymmetric wavelets have an advantage in flood flow sedimentary sequences.

Except for the influence of flows, the depositional process also has an effect over CWT. The sequence E2 and D3 formed FUCS (Fig. 9c), which is a sequence boundary belonging to the CUCS in low sequence view. That is a normal sedimentary characteristic. However, the CWT amplifies the FUCS on a small scale to cause a conflict interpretation between small scale and big scale.

6. Conclusions

(1) The results of CWT, scalogram and coefficient, are all effective methods that can be used for sequence stratigraphy analysis, in which scalogram is highly robust to noise and

coefficient has an advantage in high-frequency sequence boundaries detection. The sym4 wavelet is the best for identifying fifth-order sequence, and even partly six-order sequence, and is more sensitive to the sediment deposition by flood flows which are normal fining-upwards cycle sequences.
(2) The high-frequency sequence analysis of wavelet can be applied to construct the fine stratigraphic framework where steep-slope gravity flows deposits developed. The IPD is an effective method used to identify the proper scale for sequence detection where can be used in coarse-grained gravity flow deposits. Coefficient amplitude tendency is effective to determine the sequence boundary and discriminate the sedimentary cycle patterns in high-frequency sequence analysis. The asymmetric wavelets can detect changes at small scales in power distribution and are more sensitive to the high-frequency depositional process.
(3) The asymmetry of wavelet is the first principle, and the match with the sequence is second principle in the high-frequency sequence analysis. And the correlation of time-frequency impacts the accuracy of sequence surface localization. Several weak side lobes are the third application principle, which is useful in fifth and sixth-order sequence boundaries detection. Noise process is necessary when the SRN of data is less than 24 dB.
(4) The depositional flows, depositional process and autogenic are three sedimentary factors that affect the sequence analysis results. The sequences deposition by flood flow with finning-upwards cycles can be easily detected by asymmetric wavelets. Although the amplification of normal detail depositional characteristics by the CWT improves sequence identification accuracy; it will also produce some opposite internal sequence determination results.

Data availability statement

All data that support the findings of this study are included in this manuscript and its supplementary information files.

Declaration of interest statement

We declare that we have no financial and personal relationships with other people or organizations that can inappropriately influence our work, there is no professional or other personal interest of any nature or kind in any product, service and/or company that could be construed as influencing the position presented in, or the review of, the manuscript entitled.

CRediT authorship contribution statement

Ling Li: Concept and design, Data collection and analysis, Drafting of the article. **Zhi-Zhang Wang:** Supervision, Critical revision of the article for important intellectual content. **Shun-De Yin:** Data collection and analysis, Critical revision of the article for important intellectual content. **Wei-Fang Wang:** Data collection and analysis. **Zhi-Chao Yu:** Drafting of the article. **Wen-Tian Fan:** Drafting of the article. **Zhi-Heng Zhang:** Drafting of the article, All the authors approved the final article.

References

Akhilesh, K.V., 2012. Detecting stratigraphic discontinuities using wavelet and S-transform analysis of well log data. Geoconvention, 2012.
Andreas, P., Frederik, P.A., 2000. Wavelet analysis of well-logging data from oil source rock, Egret Member, offshore eastern Canada. Bulletin 84. https://doi.org/10.1306/8626BF15-173B-11D7-8645000102C1865D.
Arabjamaloei, R., Edalatkha, S., Jamshidi, E., Nabaei, M., Beidokhti, M., Azad, M., 2011. Exact lithologic boundary detection based on wavelet transform analysis and real-time investigation of facies discontinuities using drilling data. Petrol. Sci. Technol. 29, 569–578. https://doi.org/10.1080/10916460903419206.
Cao, Y., Wang, Y., Gluyas, J.G., Liu, Huimin, Liu, Haining, Song, M., 2018. Depositional model for lacustrine nearshore subaqueous fans in a rift basin: the eocene Shahejie Formation, dongying sag, Bohai Bay Basin, China. Sedimentology 65, 2117–2148. https://doi.org/10.1111/sed.12459.
Chandrasekhar, E., Eswara Rao, V., 2012. Wavelet analysis of geophysical well-log data of Bombay Offshore Basin, India. Math. Geosci. 44, 901–928. https://doi.org/10.1007/s11004-012-9423-4.
Choudhury, S., Chandrasekhar, E., Pandey, V.K., Prasad, M., 2007. Use of wavelet transformation for geophysical well-log data analysis. In: 2007 15th International Conference on Digital Signal Processing. Presented at the 2007 15th International Conference on Digital Signal Processing, pp. 647–650. https://doi.org/10.1109/ICDSP.2007.4288665. IEEE, Cardiff, UK.
Daubechies, I., 1990. The wavelet transform, time-frequency localization and signal analysis. IEEE Trans. Inf. Theor. 36, 961–1005. https://doi.org/10.1109/18.57199.
Deng, Q., Hu, M., Kane, O.I., Cai, Q., Hu, Z., Yang, W., 2021. Syn-rift sedimentary evolution and hydrocarbon reservoir models in a graben rift sag, Songliao Basin, Northeast China. Mar. Petrol. Geol. 132, 105245. https://doi.org/10.1016/j.marpetgeo.2021.105245.
Elkurdy, S., 2019. Extracting Seismic Stratigraphic Features Using HHT 2019, pp. 1–5. https://doi.org/10.3997/2214-4609.201977042.
Falahatkhah, O., Kordi, M., Fatemi, V., Koochi, H.H., 2021. Recognition of Milankovitch cycles during the oligocene–early miocene in the zagros basin, SW Iran: implications for paleoclimate and sequence stratigraphy. Sediment. Geol. 421, 105957. https://doi.org/10.1016/j.sedgeo.2021.105957.
Fang, W.J., Fan, Y.R., Deng, S.G., Li, X., 2007. Application of Gauss wavelet to demarcate log stratigraphic sequence automatically. J. China Univ Petrol 31 (2), 55–59. https://doi.org/10.3321/j.issn:1000-5870.2007.02.011 (in Chinese).
Fu, G.M., Zheng, R.C., Zhao, J.X., Li, Y.J., 2005. High resolution sequence stratigraphic characteristics of Yanan formation in huanxian county of Ordos basin. Acta. Sedimentol. Sin 3, 394–399. https://doi.org/10.3321/j.issn:1000-1964.2005.03.027 (in Chinese).
Ge, J., Zhao, X., Tan, M., Zhuo, H., Liu, C., Jones, B.G., 2022. Sequence stratigraphy and depositional evolution of the north-eastern shelf (33.9–10.5 ma) of the pearl river mouth basin, south China sea. Mar. Petrol. Geol. 141, 105697. https://doi.org/10.1016/j.marpetgeo.2022.105697.
Grossmann, A., Morlet, J., 1984. Decomposition of hardy functions into square integrable wavelets of constant shape. SIAM J. Math. Anal. 15, 723–736. https://doi.org/10.1137/0515056.
Guido, R.C., 2017. Effectively interpreting discrete wavelet transformed signals [Lecture Notes]. IEEE Signal Process. Mag. 34, 89–100. https://doi.org/10.1109/MSP.2017.2672759.
Guido, R.C., 2022. Wavelets behind the scenes: practical aspects, insights, and perspectives. Phys. Rep. 985, 1–23. https://doi.org/10.1016/j.physrep.2022.08.001.
Guido, R.C., Pedroso, F., Furlan, A., Contreras, R.C., Caobianco, L.G., Neto, J.S., 2020. Cwt × DWT × DTWT × SDTWT: clarifying terminologies and roles of different types of wavelet transforms. Int. J. Wavelets, Multiresolut. Inf. Process. 18, 2030001. https://doi.org/10.1142/S0219691320300017.
Huang, J., Gao, L., Gao, Y., 2007. Side lobes of wavelets impact identification of thin sand bodies. Appl. Geophys. 4, 111–117. https://doi.org/10.1007/s11770-007-0016-9.
Ji, D.W., Li, J., Lu, G.D., 2013. Application of wavelet transform in high-resolution sequence stratigraphic division. AMR (Adv. Magn. Reson.) 772, 823–827. https://doi.org/10.4028/www.scientific.net/AMR.772.823.
Kadkhodaie, A., Rezaee, R., 2017. Intelligent sequence stratigraphy through a wavelet-based decomposition of well log data. J. Nat. Gas Sci. Eng. 40, 38–50. https://doi.org/10.1016/j.jngse.2017.02.010.
Karslı, H., Dondurur, D., 2013. A procedure to reduce side lobes of reflection wavelets: a contribution to low frequency information. J. Appl. Geophys. 96, 107–118. https://doi.org/10.1016/j.jappgeo.2013.07.002.
Kulesh, M., Holschneider, M., Diallo, M.S., 2008. Geophysical wavelet library: applications of the continuous wavelet transform to the polarization and dispersion analysis of signals. Comput. Geosci. 34, 1732–1752. https://doi.org/10.1016/j.cageo.2008.03.004.
Lampe, C., Song, G., Cong, L., Mu, X., 2012. Fault control on hydrocarbon migration and accumulation in the Tertiary Dongying depression, Bohai Basin, China. AAPG Bull. 96, 983–1000. https://doi.org/10.1306/11031109023.
Li, J., Liu, Z., Liu, J., Chen, L., Liu, H., Huang, L., Qian, L., Lu, K., Liu, K., 2021. Transformation of sediment delivery and dispersal patterns controlled by relay-ramp evolution along the boundary fault of a lacustrine rift: the Eocene Shahejie formation, Dongying Sag, Bohai Bay Basin, NE China. Mar. Petrol. Geol. 128, 105044. https://doi.org/10.1016/j.marpetgeo.2021.105044.
Li, Y., Zhang, J., Xu, Y., Chen, T., Yan, X., Sun, L., Tian, W., 2022. Genetic mechanism and grading assessment of the glutenite reservoirs in the eocene Shahejie Formation, chezhen sag, Bohai Bay Basin. J. Petrol. Sci. Eng. 211, 110226. https://doi.org/10.1016/j.petrol.2022.110226.
Li, Z.D., Liu, S., Wang, H.S., 2013. Application of wavelet time frequency transform in strata sequence division——take XB areas as an example. Prog. Geophys. 29 (2), 774–779. https://doi.org/10.6038/pg20140241.
Li, Z., Yang, W., Wang, Y., Zhang, Liqiang, Luo, H., Liu, S., Zhang, Likuan, Luo, X., 2019.

Anatomy of a lacustrine stratigraphic sequence within the fourth member of the Eocene Shahejie Formation along the steep margin of the Dongying depression, eastern China. Bulletin 103, 469–504. https://doi.org/10.1306/08031817307.
Liang, J., Wang, H., Blum, M.J., Ji, X., 2019. Demarcation and correlation of stratigraphic sequences using wavelet and Hilbert-Huang transforms: a case study from Niger Delta Basin. J. Petrol. Sci. Eng. 182, 106329. https://doi.org/10.1016/j.petrol.2019.106329.
Liao, Y., Zheng, R.C., Wang, C.Y., Wang, H.H., Han, Y.L., Wang, C.Y., 2010. Analysis of high-resolution sequence stratigraphy in Chang-8 subsection of Yanchang formation, Jiyuan area of Ordos basin. Acta. Sedimentol. Sin 28, 481–488. https://doi.org/10.14027/j.cnki.cjxb.2010.03.026 (in Chinese).
Liu, H., Jiang, Z., 2010. Wavelet transform of geophysical well logging signal and its application to sequence division. In: 2010 3rd International Congress on Image and Signal Processing. Presented at the 2010 3rd International Congress on Image and Signal Processing (CISP). IEEE, Yantai, China, pp. 3470–3473. https://doi.org/10.1109/CISP.2010.5646751.
Mukherjee, B., Srivardhan, V., Roy, P., 2016. Identification of formation interfaces by using wavelet and Fourier transforms. J. Appl. Geophysics. 128, 140–149. https://doi.org/10.1016/j.jappgeo.2016.03.025.
Oliveira Santos, J.A., Uhlein, A., Dantas, M., De Morais Coutinho, G., Spier, T.J., Masse Vieira, K.H., Trindade Prado, A.C., Macharet, D., Uhlein, G.J., Novo, T., Reis, H., Farias, F.A., Freire, E.B., Carnier Fragoso, D.G., 2023. Constructing high-resolution stratigraphic frameworks by the application of signal analysis techniques: example of Balbuena IV sequence, Yacoraite formation, Salta Basin. Mar. Petrol. Geol. 157, 106470. https://doi.org/10.1016/j.marpetgeo.2023.106470.
Pan, S.-Y., Hsieh, B.-Z., Lu, M.-T., Lin, Z.-S., 2008. Identification of stratigraphic formation interfaces using wavelet and Fourier transforms. Comput. Geosci. 34, 77–92. https://doi.org/10.1016/j.cageo.2007.01.002.
Prokoph, A., Agterberg, F.P., 1999. Detection of sedimentary cyclicity and stratigraphic completeness by wavelet analysis: an application to late Albian cyclostratigraphy of the western Cananda sedimentary basin. J. Sediment. Res. 4 (26), 862–875. https://doi.org/10.1306/D4268AA9-2B26-11D7-8648000102C1865D.
Prokoph, A., Agterberg, F.P., 2000. Wavelet analysis of well-logging data from oil source rock, Egret Member, Offshore Eastern Canada. AAPG Bull. 84, 1617–1632. https://doi.org/10.1306/8626BF15-173B-11D7-8645000102C1865D.
Ren, J.F., Liao, Y.T., Sun, M., Zhao, S., Liu, X.L., Song, G.Z., 2013. A method for quantitative division of sequence stratigraphy with high-resolution based on wavelet transform and its application. Prog. Geophys. 28 (5), 2651–2658. https://doi.org/10.6038/pg20130546.
Richard, V., Brac, J., 1988. Wavelet analysis using well log information. In: SEG Technical Program Expanded Abstracts 1988. Presented at the SEG Technical Program Expanded Abstracts 1988. Society of Exploration Geophysicists, pp. 946–949. https://doi.org/10.1190/1.1892398.
Rioul, O, Vetterli, M, 1991. Wavelets and signal processing. IEEE Signal Process. Mag. 8, 14–38. https://doi.org/10.1109/79.91217.
Rivera, N.A., Ray, S., Jensen, J.L., Chan, A.K., Ayers, W.B., 2004. Detection of cyclic patterns using wavelets: an example study in the Ormskirk Sandstone, Irish Sea. Math. Geol. 36, 529–543. https://doi.org/10.1023/B:MATG.0000037735.34280.42.
Shao, X., 2017. Glutenite bodies sequence division of the upper Es4 in northern Minfeng zone of dongying sag, Bohai Bay Basin, China. In: EGU General Assembly Conference Abstracts. EGU General Assembly Conference Abstracts, p. 7394.
Shi, N., 2009. The Glutenite Bodies Depositional Stage Fine Division of the Upper Fourth Member of the Sha He Jie Sand Formation in Yan Jia-Yong an Zone. Ocean University of China (in Chinese).
Song, M.S., Li, C.L., Zhang, J.L., 2012. Fine division and correlation of conglomerate sedimentary cycles in Yanjia area of dongying depression. Acta Pet. Sin. 33 (5), 781–789. https://doi.org/10.7623/syxb201205006 (in Chinese).
Srivardhan, V., 2016. Stratigraphic correlation of wells using discrete wavelet transform with fourier transform and multi-scale analysis. Geomech. Geophys. Geo-energ. Geo-resour. 2, 137–150. https://doi.org/10.1007/s40948-016-0027-1.
Strang, G., 1993. Wavelet transforms versus Fourier transforms. Bull. Am. Math. Soc. 28, 288–305. https://doi.org/10.1090/S0273-0979-1993-00390-2.
Wang, X., 2010. Logging sequence comparison and lithologic identification study on deep sandy-conglomerate of Dongying Northern Zone. China University Of Petroleum, Qing, Dao, pp. 14–22. https://doi.org/10.7666/d.y1778025 (in Chinese).
Wang, G.W., Deng, Q.P., Tang, W.Q., 2002. The application of spectral analysis of logs in depositional cycle studies. Petrol. Explor. Dev. 29, 93–95. https://doi.org/10.0000/1000-0747-29-450.
Weedon, G.P., 2005. Time-series Analysis and Cyclostratigraphy: Examining Stratigraphic Records of Environmental Cycles. Cambridge University Press, Cambridge, pp. 64–90. https://doi.org/10.1017/CBO9780511535482.
Wei, Q.L., Zheng, R.C., Xiao, L., 2010. High-resolution sequence stratigraphy and reservoir distribution of the paleogene Zhuhai and Enping formation in the Huizhou depression. Journal of Stratigraphy 34, 60–68. https://doi.org/10.19839/j.cnki.dcxzz.2010.01.011 (in Chinese).
Wu, W., Li, Q., Pei, J., Ning, S., Tong, L., Liu, W., Feng, Z., 2020. Seismic sedimentology, facies analyses, and high-quality reservoir predictions in fan deltas: a case study of the Triassic Baikouquan Formation on the western slope of the Mahu Sag in China's Junggar Basin. Mar. Petrol. Geol. 120, 104546. https://doi.org/10.1016/j.marpetgeo.2020.104546.
Xia, L., Yiren, F., Shaogui, D., Tongshan, W., 2009. Automatic demarcation of sequence stratigraphy using the method of well logging multiscale data fusion. Petrol. Explor. Dev. 36, 221–227. https://doi.org/10.1016/S1876-3804(09)60122-1.
Xian, B.Z., Wang, Y.S., Zhou, Y.Q., Sun, L.D., 2007. Distribution and controlling factors of glutinite bodies in the actic regioin of a rift basin: an example from hezhen Sag, Bohai Bay Basin. Petrelem Explor. Dev. 34 (4), 429–436. https://doi.org/10.1016/S1872-5813(07)60034-6.
Xiao, G., Chen, J., 2003. Oil and gas in Neogene of the Bohai Sea area. Mar. Geol. Front 19, 1–6. https://doi.org/10.3969/j.issn.1009-2722.2003.08.002 (in Chinese).
Xie, R.J., Qi, J.F., Wang, Y.S., Yang, Q., 2004. Characteristics of the Cenzoic structural evolution in the north of the Dongying Sag. Pet. Explor. Dev. 26, 427–431. https://doi.org/10.11781/sysydz200405427 (in Chinese).
Xu, S., Hao, F., Xu, C., Zou, H., Zhang, X., Zhang, Y., Gao, B., Wang, Q., 2018. Gravity-flow deposits and their exploration prospects in the oligocene dongying formation, northwestern bozhong subbasin, Bohai Bay Basin, China. Mar. Petrol. Geol. 96, 179–189. https://doi.org/10.1016/j.marpetgeo.2018.06.001.
Yang, T., Cao, Y., Liu, K., Tian, J., Carlos, Z., Wang, Y., 2020. Gravity-flow deposits caused by different initiation processes in a deep-lake system. Bulletin 104, 1463–1499. https://doi.org/10.1306/03172017081.
Yang, T., Cao, Y., Liu, K., Wang, Y., Zavala, C., Friis, H., Song, M., Yuan, G., Liang, C., Xi, K., Wang, J., 2019. Genesis and depositional model of subaqueous sediment gravity-flow deposits in a lacustrine rift basin as exemplified by the Eocene Shahejie Formation in the Jiyang Depression, Eastern China. Mar. Petrol. Geol. 102, 231–257. https://doi.org/10.1016/j.marpetgeo.2018.12.033.
Yang, Y., Chen, S., Dai, C., Wang, Xiujiao, Li, X., Zeng, Q., Jiang, R., Wang, Xiaodan, Luo, Y., 2022. Prediction of glutenite reservoirs using an adaptive Bayesian seismic inversion in the slope zone of Mahu Depression in Junggar Basin, NW China. Unconv. Resour. 2, 21–30. https://doi.org/10.1016/j.uncres.2022.06.002.
Yu, Z., Wang, Z., Wang, J., 2023. Continuous wavelet transform and dynamic time warping-based fine division and correlation of glutenite sedimentary cycles. Math. Geosci. 55, 521–539. https://doi.org/10.1007/s11004-022-10039-5.
Zhang, J., Gao, J., Wu, J., Lyu, Q., Fang, D., 2019. Sedimentary characteristics and seismic geomorphology of the upper third member of Eocene Dongying Formation in double slope systems of Laoyemiao transverse anticline, Nanpu Sag, Bohai Bay Basin, China. Mar. Petrol. Geol. 109, 36–55. https://doi.org/10.1016/j.marpetgeo.2019.06.005.
Zhang, J., Song, A., 2010. Application of wavelet analysis in sequence stratigraphic division of glutenite sediments. In: 2010 International Conference on Challenges in Environmental Science and Computer Engineering. Presented at the 2010 International Conference on Challenges in Environmental Science and Computer Engineering. IEEE, Wuhan, China, pp. 204–207. https://doi.org/10.1109/CESCE.2010.69.
Zhang, Z., Zhu, X., Zhang, R., Li, Q., Shen, M., Zhang, J., 2020. To establish a sequence stratigraphy in lacustrine rift basin: a 3D seismic case study from paleogene Baxian Sag in Bohai Bay Basin, China. Mar. Petrol. Geol. 120, 104505. https://doi.org/10.1016/j.marpetgeo.2020.104505.
Zheng, R.C., Peng, J., 2002. Analysis and isochronostratigraphic correlation of high-resolution sequence stratigraphy for chang-6 oil reservoir set in Zhidan delta, northern Ordos basin. Acta. Sedimentol. Sin. 1, 92–100. https://doi.org/10.3969/j.issn.1000-0550.2002.01.016 (in Chinese).
Zheng, R.C., Peng, J., Peng, G.M., Pan, C.L., Gao, H.C., 2003. Analysis of high-resolution sequence stratigraphy of the second member of Nadu formation in Lun-35 block of baise basin and its application in development of oil reservoir. Acta. Sedimentol. Sin. 4, 654–662. https://doi.org/10.3969/j.issn.1000-0550.2003.04.018 (in Chinese).
Zhu, X., Pan, R., Li, S., Wang, H., Zhang, X., Ge, J., Lu, Z., 2018. Seismic sedimentology of sand-gravel bodies on the steep slope of rift basins — a case study of the Shahejie Formation, Dongying Sag, Eastern China. Interpretation 2 (6), 13–27. https://doi.org/10.1190/INT-2017-0154.1.